

Magnetoelastic coupling of MnAs/GaAs(001) close to the phase transition

R. Koch,* C. Pampuch,† H. Yamaguchi,‡ A. K. Das,§ A. Ney,|| L. Däweritz, and K. H. Ploog
Paul-Drude-Institut für Festkörperelektronik, Hausvogteiplatz 5-7, D-10117 Berlin

(Received 7 June 2004; published 22 September 2004)

The magnetoelastic coupling of epitaxial MnAs films on GaAs(001) has been investigated with a sensitive cantilever beam magnetometer. We find that even at 10 °C, i.e., very close to the combined structural and magnetic phase transition from α - to β -MnAs (10–40 °C), the magnetoelastic coupling constants are comparable in magnitude with the small values of the 3d ferromagnets. The coupling is largest within the hexagonal plane of MnAs, described by constant B_1 , rather than along the c -axis, where the Mn atoms are nearest neighbors. Our experimental results, therefore, support an indirect exchange mechanism via the Mn-As-Mn bonds in accordance with pair model calculations.

DOI: 10.1103/PhysRevB.70.092406

PACS number(s): 75.70.Ak, 68.60.Bs, 75.80.+q

I. INTRODUCTION

Magnetostriction is the property of magnetic materials to change the lattice dimensions when the state of magnetization varies^{1,2}—a phenomenon well-known, e.g., from the droning of transformers. In the phenomenological description of thermodynamics, magnetostriction is represented by an awkward fourth-rank tensor that accounts for the simultaneous dependence of the free energy (enthalpy) on magnetization and strain (stress).^{3,4} Since—in contrast to the quadratic elastic energy—the dependence on strain (stress) is linear, “magnetoelastic” (ME) energy may be gained by slightly distorting the crystal lattice. Typically, magnetostrictive distortions are very small ($\lambda \sim 10^{-5}$ – 10^{-4}), corresponding only to minute energies of 0.01–0.1 $\mu\text{eV}/\text{atom}$. For comparison, the magnetocrystalline anisotropy (MCA), which commonly is responsible for the occurrence of easy and hard magnetization axes, has energies of the order of $\sim 10 \mu\text{eV}/\text{atom}$.

The origin of magnetostriction (like the MCA energy) essentially lies in the spin-orbit coupling, which interrelates spin orientation and chemical bonding. Two different theoretical approaches are established to understand the ME coupling constants in terms of an atomic scale picture. The first one concerns substances with a localized magnetism,² where models based on pair interactions^{5,6} were employed successfully to describe and understand the experimental data. The second approach treats magnetoelasticity in the framework of band theory and is particularly suitable for magnetic materials with itinerant electrons. However, due to the small energies involved, magnetoelastic effects became accessible to modern first principle calculations only recently. Good agreement with experiment was achieved by calculating the ME coupling constants with density functional theory, e.g., of the transition metals Fe,^{7,8} Co,^{9–11} and Ni^{10,12} as well as of the rare earth metals Er and Tb.¹³ But since the number of nearest neighbors in these systems is very large (12 for fcc and hcp and 8 for bcc), a straightforward correlation with atomic properties is difficult. It is noteworthy that pair models—though being not really suitable—give reasonable values for the surface anisotropy of transition metals.^{14,15}

Here we present a quantitative investigation of the magnetoelastic coupling constants of α -MnAs, which is an inter-

esting magnetic material in many respects: (i) α -MnAs crystallizes in the hexagonal NiAs structure^{16,17} with alternating hexagonal planes of Mn and As atoms [Fig. 1(a)]. The spin moments are carried mainly by the Mn ions, each of them exhibiting two types of magnetic neighbors: Two first-nearest neighbors along the c -axis at a distance of $c/2=0.286$ nm and six second-nearest neighbors within the hexagonal plane at a distance of $a=0.370$ nm. (ii) Contrary to Co, the easy axis of magnetization lies along the a -axis¹⁸ with an anisotropy field as large as 2.1 T in direction of the c -axis.^{19,20} (iii) There is increasing evidence, that ferromagnetic ordering is mainly transmitted by the strongly directional and localized Mn-As-Mn bonds via a double-exchange mechanism.^{21–23} (iv) On the other hand, α -MnAs shows metallic conductivity,²⁴ thus containing itinerant electrons.²⁵ (v) α -MnAs undergoes a simultaneous first-order structural and magnetic phase transition to the paramagnetic β -MnAs; in the bulk the transition proceeds at about 40 °C,¹⁶ in the case of MnAs/GaAs(001) films a strain-stabilized pattern of co-existing α - and β -MnAs stripes along the c axis is formed in the temperature range of 10–40 °C.^{26,27} By relating the experimental ME coupling to a pair interaction model our study reveals that the Mn atoms along the c -axis—though being the first-nearest neighbors—play at best a minor role for the exchange coupling. The ferromagnetic ordering within and in between the hexagonal Mn planes seems to be transmitted by the Mn-As-Mn bonds, thus supporting a localized rather than an itinerant magnetism.

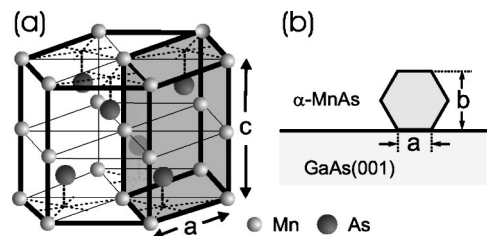


FIG. 1. (a) NiAs-type crystal structure of α -MnAs consisting of hexagonal planes of Mn and As alternating in a sequence ABAC... (b) Epitaxial configuration of MnAs/GaAs(001) with the a - and c -axis of MnAs oriented parallel to GaAs[110] and GaAs[1 $\bar{1}$ 0], respectively.

II. DESIGN OF EXPERIMENT

The complete set of ME coupling constants B_1 , B_2 , B_3 , and B_4 , presented here, was determined by means of 60 nm-thick, high-quality single-crystalline α -MnAs films on GaAs(001). The MnAs films were prepared by molecular beam epitaxy on commercial, 100 μm thick, epi-ready GaAs(001) wafers as described in detail elsewhere.^{28,29} Under the chosen conditions, MnAs grows predominantly (95%) in its A -orientation with MnAs($\bar{1}100$) plane parallel to the substrate surface and MnAs[0001] \parallel GaAs[$1\bar{1}0$].³⁰ The film contains only small amounts of MnAs in the B -orientation (rotated by 90° in-plane)³⁰ as well as a tiny fraction with an out-of-plane magnetization.³¹ The magnetic measurements were performed with a sensitive cantilever beam magnetometer (CBM).³² As cantilever beam substrates we cut $25 \times 5 \text{ mm}^2$ sized samples with GaAs[110], GaAs[$1\bar{1}0$] or GaAs[100] directed along the length (see below), and the film covering an area of $11 \times 5 \text{ mm}^2$. The presented experimental data have been determined at 10°C , i.e., in the pure α -phase very close to the phase transition temperature;²³ identical results are obtained at 0°C .

For the evaluation of our experimental data we derived the general equations of the elastic energy F_{el} and the ME energy F_{me1} of hexagonal materials by Legendre transformation of the respective expression for the free enthalpy given by Mason⁴ and obtain

$$F_{\text{el}} = \frac{1}{2}c_{11}(\epsilon_1^2 + \epsilon_2^2) + c_{12}\epsilon_1\epsilon_2 + c_{13}\epsilon_3(\epsilon_1 + \epsilon_2) + \frac{1}{2}c_{33}\epsilon_3^2 + \frac{1}{2}c_{44}(\epsilon_4^2 + \epsilon_5^2) + \frac{1}{4}(c_{11} - c_{12})\epsilon_6^2, \quad (1)$$

$$F_{\text{me1}} = B_1[\alpha_1^2\epsilon_1 + \alpha_2^2\epsilon_2 + \alpha_1\alpha_2\epsilon_6] - B_2\alpha_3^2\epsilon_3 - B_3\alpha_3^2(\epsilon_1 + \epsilon_2) + B_4(\alpha_2\alpha_3\epsilon_4 + \alpha_1\alpha_3\epsilon_5). \quad (2)$$

Here the ϵ_i represent the strain in Voigt's notation, the α_i are the direction cosines of magnetization with respect to the hexagonal lattice, c_{ij} and B_i denote the elastic constants and the ME coupling constants, respectively. Subtracting the energy of the demagnetized state of MnAs, i.e., $\alpha_1=1$, $\alpha_2=\alpha_3=0$, yields

$$F_{\text{me1}} = B_1[(\alpha_1^2 - 1)\epsilon_1 + \alpha_2^2\epsilon_2 + \alpha_1\alpha_2\epsilon_6] - B_2\alpha_3^2\epsilon_3 - B_3\alpha_3^2(\epsilon_1 + \epsilon_2) + B_4(\alpha_2\alpha_3\epsilon_4 + \alpha_1\alpha_3\epsilon_5). \quad (3)$$

Note that Eq. (3) differs from the free energy of Co^{14,33} due to the different demagnetized state, since the easy magnetization direction of the MnAs film lies along the a -axis and not the c -axis. The obtained negative signs are introduced for consistency with Co and essentially yield the same relation between the ME coupling constants (B_1 , B_2 , B_3 , B_4) and the magnetostrictive constants (λ_A , λ_B , λ_C , λ_D).³⁴ However, the term $B_1\alpha_1\alpha_2\epsilon_6$ in Eq. (3) differs by a factor of 2 from respective term of Co,³³ probably due to an error upon interconverting tensor and Voigt notations.^{14,33}

For measuring B_1 and B_3 the MnAs[$11\bar{2}0$] direction (a -axis in the film plane) was chosen to be parallel to the length of the cantilever beam. In that geometry the difference

TABLE I. Experimental magnetostrictive stress at 10°C , corresponding ME coupling and magnetostrictive constants of MnAs, as well as the resulting parameters of the pair model.

$\Delta\sigma_i^j$ (MJ/m ³)	B_i (MJ/m ³)	λ_i (10 ⁻⁶) ^a	Pair-model (MJ/m ³)	
$\sigma_1^b - \sigma_1^a$	+8.2	B_1 -6.6	λ_A +182	s_1 -0.9
$\sigma_1^c - \sigma_1^a$	+8.1	B_2 +0.4	λ_B +3	$r_1 t_1$ -7.1
$\sigma_3^c - \sigma_3^a$	-1.0	B_3 -2.0	λ_C -25	s_2 +2.6
$\sigma_{45^\circ}^j - \sigma_{45^\circ}^a$	+3.0	B_4 +1.3	λ_D +30	$r_2 t_2$ -0.4

^aElastic constants taken from Ref. 35.

in magnetostrictive stress upon saturating the magnetization along the b -axis (i.e., perpendicular the film, denoted by σ_1^b) and along the a -axis in the film plane (σ_1^a) yields B_1 , i.e., $\sigma_1^b - \sigma_1^a = -B_1(1 + c_{12}/c_{11})$. Saturating the magnetization along the c -axis gives $\sigma_1^c - \sigma_1^a = -B_1 - B_3(1 - c_{12}/c_{11})$. For measurement of B_2 the stress is measured along MnAs[0001], i.e., the c -axis parallel to the length of the cantilever beam, with $\sigma_3^c - \sigma_3^a = -B_2 + (c_{13}/c_{11})B_3$. We remark that for both geometries a $\langle 100 \rangle$ direction of the GaAs(001) substrate is parallel to the length of the cantilever beam. Since the respective Poisson ratio $\nu \approx 0$, the involved Poisson stress is negligible. In order to determine B_4 the GaAs(001) substrate was cut along the [100] direction, i.e., a - and c -axes of MnAs azimuthally rotated by 45° compared to the preceding cases. Magnetizing the MnAs film along the cantilever beam axis (denoted by l) yields $\sigma_{45^\circ}^j - \sigma_{45^\circ}^a = -\{B_1 + B_2 + [1 - (c_{12} + c_{13})/c_{11}]B_3\}/4 - [(\nu + 1)/(\nu - 1)]B_4$ from which B_4 is obtained.

III. EXPERIMENTAL RESULTS

The experimental stress measured by CBM as well as the obtained ME coupling constants of MnAs are listed in Table I. We also include the corresponding magnetostrictive constants which are calculated from the experimental B_i values and using the elastic constants of Ref. 35. From the sets of constants we conclude that the ME coupling in α -MnAs, even very close to the combined structural and magnetic phase transition, is not extraordinarily high. In fact, the magnitude of the B_i is of the same order as the small values of the transition metals Fe, Co, and Ni. The ME coupling is largest within the hexagonal plane of MnAs, which is described by the constant B_1 , and not along the c -axis, where the Mn atoms are nearest neighbors. B_1 is negative, implying that ME energy is gained upon expansion as well as shearing of the hexagonal plane. Obviously, from a ME point of view an even larger unit cell is favored. Straining along as well as shearing with respect to the c -axis, on the other hand, have less influence.

IV. PAIR INTERACTION CALCULATIONS

In order to gain deeper insight into the magnetic properties of MnAs from its ME coupling behavior, we approximate the exchange interaction by a pair model introduced

originally by Néel.³⁷ In this model (see also Ref. 14) the magnetocrystalline energy is assumed to be the sum of two-body terms w_{ij} that can be expanded in Legendre polynomials (P_i)

$$w_{ij}(r_{ij}\phi) = f_2(r_{ij})P_2(\cos \phi) + f_4(r_{ij})P_4(\cos \phi) + \dots \\ \simeq f_2(r_{ij})\left(\cos^2 \phi - \frac{1}{3}\right), \quad (4)$$

ϕ denotes the angle between the magnetization vector and the bond axis of atoms i and j , the $f_n(r_{ij})$ are functions of the respective interatomic distance r_{ij} . For simplicity higher terms than P_2 are neglected. f_2 is developed in powers of δr_{ij} , which is the deviation of r_{ij} from the equilibrium value. First order magnetostriction is obtained by taking $f_2 \simeq s_j + t_j \delta r_{ij}$. Then the energy w_i of atom i is given by

$$w_i = \frac{1}{2} \sum_j \left[t_j \delta r_{ij} \left(\cos^2 \phi - \frac{1}{3} \right) + s_j \delta (\cos^2 \phi) \right]. \quad (5)$$

The summation is performed over the nearest neighbors of atom i . For MnAs we consider two different types of neighbors, namely the six neighboring Mn atoms within the hexagonal plane (type 1, $r_1=0.37$ nm) and the two nearest neighbor Mn atoms along the c -axis (type 2, $r_2=0.286$ nm). Note that $t_j \delta r_{ij}$ can be expressed as a function of the strain components ($t_j r_{ij} \epsilon_{mn}$), i.e., $t_j r_{ij}$ being the parameter which accounts for the magnetostrictive straining in the pair-model. In order to relate the parameters s_j and t_j to the ME coupling constants B_i of Eq. (3) we followed the derivation discussed in detail in Ref. 14 and obtain for our system:

$$s_1 = \frac{1}{3}(B_1 - 2B_3), \\ r_1 t_1 = \frac{2}{3}(B_1 + 2B_3), \\ s_2 = \frac{1}{2}(-B_1 + 2B_3 + 2B_4), \\ r_2 t_2 = -B_2. \quad (6)$$

The values of s_i and $r_i t_i$ presented in the last column of Table I were calculated with the four experimental ME coupling constants of MnAs also given in Table I. It is notable that the pair model clearly distinguishes between the two types of Mn neighbors. The distance gradient of the pair energy is larger by a factor of almost 20 for Mn pairs in the hexagonal plane ($r_1 t_1$) than along the c -axis ($r_2 t_2$). Since the lattice spacing in the hexagonal plane definitely is too large for a direct exchange interaction—as confirmed by recent density functional theory calculations³⁸—the pair model calculations support an indirect exchange mechanism. The ME

coupling of MnAs, therefore, underlines the importance of the hexagonal plane for ferromagnetism in MnAs and further corroborates a double exchange mechanism transmitted by the As atoms located between the hexagonal Mn planes as indicated by previous studies.^{21–23} As shown in Ref. 14 the pair model provides also an estimate for the MCA energy. With the data of Table I a value of 3.9 MJ/m³ (0.83 meV/Mn) is obtained, which is in reasonable agreement with the experimental value of 0.7 MJ/m³ (0.15 meV/Mn) determined recently by ferromagnetic resonance,³⁹ particularly when considering the simplified model assumptions. The accuracy is of the same order as found for Co.¹⁴

V. SUMMARIZING DISCUSSION

We investigated the ME coupling of MnAs/GaAs(001) with our sensitive CBM. For evaluation of the experimental data, we derived the appropriate equation of the ME free energy for MnAs as well as the respective relations between magnetostrictive stress and the ME coupling constants. We found that even very close to the phase transition temperature the ME coupling constants of MnAs are comparable in magnitude with that of the 3d ferromagnets. Giant length changes as described in Ref. 36 are only observed in the phase coexistence region of α - and β -MnAs, but not in the pure α -phase. The obtained constants B_1 - B_4 actually are also valid for bulk MnAs, since interface effects can be neglected in 60 nm thick films. Furthermore, second-order ME coupling^{8,11,12,40,41} plays a minor role, since the MnAs/GaAs(001) films are nearly strain relieved at the growth temperature;⁴² in a recent study we estimated a only small residual stress of about 0.15 GPa in the α -phase at 10 °C.⁴³ Our measurements show that the ME coupling of MnAs is largest within the hexagonal planes and not along the perpendicular c -axis, where the Mn atoms are nearest neighbors. Pair model calculations reveal a distance dependence of the pair energy that is larger by a factor of ~ 20 for the Mn pairs in the hexagonal planes, thus supporting an indirect exchange mechanism. All in all, our study of MnAs with two different types of Mn neighbors represents an illustrative example for understanding the ME coupling in terms of an atomistic picture.

ACKNOWLEDGMENTS

The work was supported by the Deutsche Forschungsgemeinschaft (Sfb 290) and the NEDO International Joint Research Program “Nanoelasticity.”

*Electronic address: koch@pdi-berlin.de

†New address: Specs GmbH, Voltastraße 5, 13355 Berlin.

‡Permanent address: NTT Basic Research Laboratories, 3-1 Morinosato Wakamiya, Atsugi-shi, Kanagawa 243-0198, Japan.

§Permanent address: Department of Physics, Indian Institute of Technology, Kharagpur-721302, India.

¶Present address: Solid State and Photonics Laboratory, Stanford University, Stanford, California 94305, USA.

- ¹R. Becker and W. Döring, *Ferromagnetismus* (Springer-Verlag, Berlin, 1939).
- ²E. du Trémolet de Lacheisserie, *Magnetostriction: Theory and Applications of Magnetoelasticity* (CRC, Boca Raton, 1993).
- ³W. P. Mason, Phys. Rev. **82**, 715 (1951).
- ⁴W. P. Mason, Phys. Rev. **96**, 302 (1954).
- ⁵L. Néel, J. Phys. Radium **15**, 225 (1954).
- ⁶E. Callen and H. B. Callen, Phys. Rev. **139**, A455 (1965).
- ⁷R. Wu, L. Chen, and A. J. Freeman, J. Magn. Magn. Mater. **170**, 103 (1997).
- ⁸M. Komelj and M. Fähnle, J. Magn. Magn. Mater. **220**, L8 (2000).
- ⁹A. B. Shick, D. L. Novikov, and A. J. Freeman, J. Magn. Magn. Mater. **177–181**, 1223 (1998).
- ¹⁰G. Y. Guo, J. Magn. Magn. Mater. **209**, 33 (2000).
- ¹¹M. Komelj and M. Fähnle, J. Magn. Magn. Mater. **224**, L1 (2001).
- ¹²M. Komelj and M. Fähnle, J. Magn. Magn. Mater. **222**, L245 (2000).
- ¹³S. Buck and M. Fähnle, Phys. Rev. B **57**, R14 044 (1998).
- ¹⁴P. Bruno, J. Phys. F: Met. Phys. **18**, 1291 (1988).
- ¹⁵D. S. Chuang, C. A. Ballentine, and R. C. O'Handley, Phys. Rev. B **49**, 15 084 (1994).
- ¹⁶B. T. M. Willis and H. P. Rooksby, Proc. Phys. Soc. London **67**, 290 (1954).
- ¹⁷R. H. Wilson and J. S. Kasper, Acta Crystallogr. **17**, 95 (1964).
- ¹⁸R. W. De Blois and D. S. Rodbell, Phys. Rev. **130**, 1347 (1963).
- ¹⁹M. Tanaka, J. P. Harbison, M. C. Park, Y. S. Park, T. Shin, and G. M. Rothberg, J. Appl. Phys. **76**, 6278 (1994).
- ²⁰F. Schippan, G. Behme, L. Däweritz, K. H. Ploog, B. Dennis, K.-U. Neumann, and K. R. A. Ziebeck, J. Appl. Phys. **88**, 2766 (2000).
- ²¹N. Menyuk, J. A. Kafalas, K. Dwight, and J. B. Goodenough, Phys. Rev. **177**, 942 (1969).
- ²²K. Bärner, Phys. Status Solidi B **88**, 13 (1978).
- ²³A. K. Das, C. Pampuch, A. Ney, T. Hesjedal, L. Däweritz, R. Koch, and K. H. Ploog, Phys. Rev. Lett. **91**, 087203 (2003).
- ²⁴S. Haneda, N. Kazama, Y. Yamaguchi, and H. Watanabe, J. Phys. Soc. Jpn. **42**, 1201 (1977).
- ²⁵J. Mira, F. Rivadulla, J. Rivas, A. Fondado, T. Guidi, R. Caciuffo, F. Carsughi, P. G. Radaelli, and J. B. Goodenough, Phys. Rev. Lett. **90**, 097203 (2003).
- ²⁶V. M. Kaganer, B. Jenichen, F. Schippan, W. Braun, L. Däweritz, and K. H. Ploog, Phys. Rev. Lett. **85**, 341 (2000).
- ²⁷T. Plake, M. Ramsteiner, V. M. Kaganer, B. Jenichen, M. Kästner, L. Däweritz, and K. H. Ploog, Appl. Phys. Lett. **80**, 2523 (2002).
- ²⁸F. Schippan, A. Trampert, L. Däweritz, and K. H. Ploog, J. Vac. Sci. Technol. B **17**, 1716 (1999).
- ²⁹M. Kästner, C. Herrmann, L. Däweritz, and K. H. Ploog, J. Appl. Phys. **92**, 5711 (2002).
- ³⁰L. Däweritz, M. Ramsteiner, A. Trampert, M. Kästner, F. Schippan, H.-P. Schönherr, B. Jenichen, and K. H. Ploog, Phase Transitions **76**, 445 (2003).
- ³¹A. Ney, T. Hesjedal, C. Pampuch, J. Mohanty, A. K. Das, L. Däweritz, R. Koch, and K. H. Ploog, Appl. Phys. Lett. **83**, 2850 (2003).
- ³²M. Weber, R. Koch, and K. H. Rieder, Phys. Rev. Lett. **73**, 1166 (1994).
- ³³Th. Gutjahr-Löser, D. Sander, and J. Kirschner, J. Magn. Magn. Mater. **220**, L1 (2000).
- ³⁴Equation (1) yields the same relation between the ME coupling constants and the magnetostrictive constants for MnAs and Co (cf. Ref. 33), namely $B_1 = -(\lambda_A - \lambda_B)(c_{11} - c_{12})$, $B_2 = -(\lambda_A + \lambda_B)c_{13} - \lambda_C c_{33}$, $B_3 = -\lambda_A c_{12} - \lambda_B c_{11} - \lambda_C c_{13}$, and $B_4 = -(\lambda_A + \lambda_C - 4\lambda_D)c_{44}$.
- ³⁵M. Dörfler and K. Bärner, Phys. Status Solidi A **17**, 141 (1973).
- ³⁶V. A. Chernenko, L. Wee, P. G. McCormick, and R. Street, J. Appl. Phys. **85**, 7833 (1999).
- ³⁷L. Néel, J. Phys. Radium **15**, 225 (1954).
- ³⁸A. Continenza, S. Picozzi, W. T. Geng, and A. J. Freeman, Phys. Rev. B **64**, 085204 (2001).
- ³⁹J. Lindner, T. Tolinski, K. Lenz, E. Kosubek, H. Wende, K. Baberschke, A. Ney, T. Hesjedal, C. Pampuch, R. Koch, L. Däweritz, and K. H. Ploog, J. Magn. Magn. Mater. **277**, 159 (2004).
- ⁴⁰G. Wedler, J. Walz, A. Greuer, and R. Koch, Phys. Rev. B **60**, R11 313 (1999).
- ⁴¹D. Sander, Rep. Prog. Phys. **62**, 809 (1999).
- ⁴²A. Trampert, F. Schippan, L. Däweritz, and K. H. Ploog, Appl. Phys. Lett. **78**, 2461 (2001).
- ⁴³A. Ney, T. Hesjedal, C. Pampuch, A. K. Das, L. Däweritz, R. Koch, K. H. Ploog, T. Tolinski, J. Lindner, K. Lenz, and K. Baberschke, Phys. Rev. B **69**, 081306(R) (2004).